

RESEARCH ARTICLE

Interplay between radiation pressure force and scattered light intensity in the cooperative scattering by cold atoms

T. Bienaimé^a, R. Bachelard^b, J. Chabé^a, M. T. Rouabah^{a,c}, L. Bellando^a, Ph. W. Courteille^b, N. Piovella^d, R. Kaiser^{a *}

^a *Université de Nice Sophia Antipolis, CNRS, Institut Non-Linéaire de Nice, UMR 7335, F-06560 Valbonne, France*

^b *Instituto de Física de São Carlos, Universidade de São Paulo, 13560-970 São Carlos, SP, Brazil*

^c *Laboratoire de Physique Mathématique et Physique Subatomique, Université Constantine 1, Constantine 25000, Algeria*

^d *Dipartimento di Fisica, Università Degli Studi di Milano, Via Celoria 16, I-20133 Milano, Italy*

(March 20, 2013)

The interplay between the superradiant emission of a cloud of cold two-level atoms and the radiation pressure force is discussed. Using a microscopic model of coupled atomic dipoles driven by an external laser, the radiation field and the average radiation pressure force are derived. A relation between the far-field scattered intensity and the force is derived, using the optical theorem. Finally, the scaling of the sample scattering cross section with the parameters of the system is studied.

Keywords: Cold atoms, Dicke superradiance, cooperative scattering.

1. Introduction

When a single atom is illuminated by a laser, it scatters the light isotropically, up to polarization effects. The scattering process results in a force proportional to the number of photons scattered. Indeed, as an atom absorbs a photon from the laser of wave vector \mathbf{k}_0 , it acquires a momentum $\hbar\mathbf{k}_0$, but the average momentum change during the emission process is zero as it re-emits the photon in a random direction.

As a collection of atoms, the picture changes drastically as the atoms cooperate to scatter the light. The phenomenon was first identified by Dicke (1) and it was shown to lead to a directional emission of the light, due to the synchronization of the atomic dipoles with the laser. The collective effects becomes even stronger as the atomic medium becomes optically dense and the radiation of the atoms starts to alter significantly the wave propagation. Among the other collective effects that arise, one can mention the collective Lamb shift (2, 3), Mie resonances (4), as well as a reduction of the radiation pressure force (5, 6).

Since the radiated light results from the interference of the waves emitted by each dipole, the simple relation between emitted photon and atomic recoil is lost. For example, a striking feature of cooperativity is the modification of the atomic recoil due to the presence of the neighboring atoms (7, 8), an effect that cannot be deduced from single-atom physics.

We here discuss the particular relation between the directional superradiant emission, and the reduction of the radiation pressure force. The atomic cloud is described as a microscopic

*Corresponding author. Email: robin.kaiser@inln.cnrs.fr

ensemble of coupled atomic dipoles, and both the radiated field and the force are expressed as a function of these dipoles. The optical theorem is derived in this framework, and is shown to lead to a direct relation between intensity scattered and radiation pressure force for the cloud center-of-mass.

2. Cooperative scattering model

The atomic cloud is described as a system of two-level (g and e) atoms, with resonant frequency ω_a and position \mathbf{r}_j , that are driven by an uniform laser beam with electric field amplitude E_0 , frequency ω_0 and wave vector $\mathbf{k}_0 = (\omega_0/c)\hat{\mathbf{e}}_z$. The laser-atom interaction is described by the following Hamiltonian:

$$H = \frac{\hbar\Omega_0}{2} \sum_{j=1}^N \left[\hat{\sigma}_j e^{i(\Delta_0 t - \mathbf{k}_0 \cdot \mathbf{r}_j)} + \text{h.c.} \right] + \hbar \sum_{j=1}^N \sum_{\mathbf{k}} g_{\mathbf{k}} \left(\hat{\sigma}_j e^{-i\omega_a t} + \hat{\sigma}_j^\dagger e^{i\omega_a t} \right) \left[\hat{a}_{\mathbf{k}}^\dagger e^{i(\omega_{\mathbf{k}} t - \mathbf{k} \cdot \mathbf{r}_j)} + \hat{a}_{\mathbf{k}} e^{-i(\omega_{\mathbf{k}} t - \mathbf{k} \cdot \mathbf{r}_j)} \right] \quad (1)$$

where $\Omega_0 = dE_0/\hbar$ is the Rabi frequency of the incident laser field and $\Delta_0 = \omega_0 - \omega_a$ is the detuning between the laser and the atomic transition. In Eq. (1) $\hat{\sigma}_j = |g_j\rangle\langle e_j|$ is the lowering operator for j -atom, $\hat{a}_{\mathbf{k}}$ is the photon annihilation operator and $g_{\mathbf{k}} = (d^2\omega_{\mathbf{k}}/2\hbar\epsilon_0 V)^{1/2}$ is the single-photon Rabi frequency, where d is the electric-dipole transition matrix element and V is the photon volume. The special case where a single photon (mode \mathbf{k}) can be assumed to be present in the system, was extensively investigated in Refs. (2, 9, 10), and later extended to include a low-intensity laser in Ref. (5, 11, 12). The system atoms+photons is then described by a state of the form (13):

$$|\Psi\rangle = \alpha(t)|g_1 \dots g_N\rangle|0\rangle_{\mathbf{k}} + e^{-i\Delta_0 t} \sum_{j=1}^N \beta_j(t)|g_1 \dots e_j \dots g_N\rangle|0\rangle_{\mathbf{k}} + \sum_{\mathbf{k}} \gamma_{\mathbf{k}}(t)|g_1 \dots g_N\rangle|1\rangle_{\mathbf{k}} + \sum_{m,n=1}^N \epsilon_{m<n,\mathbf{k}}(t)|g_1 \dots e_m \dots e_n \dots g_N\rangle|1\rangle_{\mathbf{k}}, \quad (2)$$

The first term in Eq. (2) corresponds to the initial ground state without photons, the second term is the sum over the states where a single atom has been excited by the classical field. The third term corresponds to the atoms that returned to the ground state having emitted a photon in the mode \mathbf{k} , whereas the last one corresponds to the presence of two excited atoms and one virtual photon with ‘negative’ energy. It is due to the counter-rotating terms in the Hamiltonian (1) and disappears when the rotating wave approximation is made. In the linear regime $\alpha \approx 1$ and in the Markov approximation, valid if the decay time is larger than the photon time-of-flight through the atomic cloud, the scattering problem reduces to the following differential equation (11, 12, 14)

$$\dot{\beta}_j = \left(i\Delta_0 - \frac{\Gamma}{2} \right) \beta_j - i\frac{\Omega_0}{2} e^{i\mathbf{k}_0 \cdot \mathbf{r}_j} - \frac{\Gamma}{2} \sum_{m \neq j} \frac{\exp(ik_0|\mathbf{r}_j - \mathbf{r}_m|)}{ik_0|\mathbf{r}_j - \mathbf{r}_m|} \beta_m \quad (3)$$

with initial condition $\beta_j(0) = 0$, for $j = 1, \dots, N$. Here, $\Gamma = Vg_k^2 k_0^2/\pi c = d^2 k_0^3/2\pi\epsilon_0\hbar$ is the single-atom *spontaneous* decay rate. The kernel in the last term of Eq. (3) has a real component,

$-(\Gamma/2) \sum_{m \neq j} [\sin(x_{jm})/x_{jm}]$ (where $x_{jm} = k_0|\mathbf{r}_j - \mathbf{r}_m|$), describing the *collective* atomic decay, and an imaginary component, $i(\Gamma/2) \sum_{m \neq j} [\cos(x_{jm})/x_{jm}]$, describing the collective Lamb shift (14–16). Notice that while Eq. (3) is here deduced from a quantum mechanical model, it can also be obtained classically, treating the two-level atoms as weakly excited classical harmonic oscillators (13, 17).

3. Radiated field

The radiation field operator $\hat{a}_{\mathbf{k}}$ evolves according to the following Heisenberg equation

$$\frac{d\hat{a}_{\mathbf{k}}}{dt} = \frac{1}{i\hbar} [\hat{a}_{\mathbf{k}}, \hat{H}] = -ig_k e^{i(\omega_k - \omega_a)t} \sum_{m=1}^N \hat{\sigma}_m e^{-i\mathbf{k} \cdot \mathbf{r}_m}, \quad (4)$$

where the fast oscillating term proportional to $\exp[i(\omega_k + \omega_a)t]$ has been neglected. The scattered field is obtained by performing the sum over all the modes, considering only the positive-frequency part of the electric field operator

$$\hat{E}_s(\mathbf{r}, t) = \sum_{\mathbf{k}} \mathcal{E}_k \hat{a}_{\mathbf{k}}(t) e^{i\mathbf{k} \cdot \mathbf{r} - i\omega_k t} \quad (5)$$

where $\mathcal{E}_k = (\hbar\omega_k/2\epsilon_0 V)^{1/2}$. Integrating Eq. (4) with respect to time, with $a_{\mathbf{k}}(0) = 0$, inserting it in Eq. (5), and assuming the usual Markov approximation, one obtains (12)

$$\hat{E}_s(\mathbf{r}, t) \approx -\frac{dk_0^3}{4\pi\epsilon_0} e^{-i\omega_a t} \sum_{m=1}^N \frac{e^{ik_0|\mathbf{r}-\mathbf{r}_m|}}{k_0|\mathbf{r}-\mathbf{r}_m|} \hat{\sigma}_m(t). \quad (6)$$

When applied on the state (2), neglecting virtual transitions, it yields $\hat{E}_s|\Psi\rangle = E_s \exp(-i\omega_0 t)|g_1 \dots g_N\rangle$, with

$$E_s(\mathbf{r}, t) = -\frac{\hbar\Gamma}{2d} \sum_{m=1}^N \beta_m(t) \frac{e^{ik_0|\mathbf{r}-\mathbf{r}_m|}}{k_0|\mathbf{r}-\mathbf{r}_m|} \quad (7)$$

Hence, the radiated field appears as a sum of spherical waves radiated by the atomic dipoles. In the far-field limit, one has $k_0|\mathbf{r}-\mathbf{r}_m| \approx k_0 r - \mathbf{k} \cdot \mathbf{r}_m$, with $\mathbf{k} = k_0(\mathbf{r}/r)$, so the field (7) radiated in a direction \mathbf{k} reads

$$E_s^{(\text{far})}(\mathbf{k}, t) \approx -\frac{\hbar\Gamma}{2d} \frac{e^{ik_0 r}}{k_0 r} \sum_{m=1}^N \beta_m(t) e^{-i\mathbf{k} \cdot \mathbf{r}_m}. \quad (8)$$

The emitted intensity in a direction \mathbf{k} is then derived as

$$I_s(\mathbf{k}) = \frac{\epsilon_0 c \hbar^2 \Gamma^2}{2(dk_0 r)^2} \left| \sum_{m=1}^N \beta_m(t) e^{-i\mathbf{k} \cdot \mathbf{r}_m} \right|^2 \quad (9)$$

$$= \frac{\epsilon_0 c \hbar^2 \Gamma^2}{2(dk_0 r)^2} \left(\sum_{m=1}^N |\beta_m|^2 + \sum_{j \neq m}^N \beta_j \beta_m^* e^{-i\mathbf{k} \cdot (\mathbf{r}_j - \mathbf{r}_m)} \right). \quad (10)$$

Integrating this intensity over all directions leads to a radiated power

$$P_r = \frac{d^2 k_0^4 c}{2\pi\epsilon_0} \left(\sum_{m=1}^N |\beta_m|^2 + \sum_{m \neq j}^N \beta_j \beta_m^* \frac{\sin(k_0 |\mathbf{r}_j - \mathbf{r}_m|)}{k_0 |\mathbf{r}_j - \mathbf{r}_m|} \right), \quad (11)$$

where we have used the equality

$$\int d\mathbf{k} e^{ik_0 \hat{\mathbf{k}} \cdot \mathbf{d}} = 4\pi \frac{\sin(k_0 |d|)}{k_0 |d|}. \quad (12)$$

In Eq. (11), the first term corresponds to the *incoherent* sum of the single atom radiated power. The second term is an interference term; in the limit of a cloud small compared to the wavelength, the dipole moments have the same phase and this latter term is responsible for a superradiant build-up of the radiated power $\propto N^2$ (see, e.g., Ref. (1)).

4. The radiation pressure force

As for the radiation force operator acting on the j th atom, it is derived from Eq. (1) as

$$\hat{\mathbf{F}}_j = -\nabla_{\mathbf{r}_j} \hat{H} = \hat{\mathbf{F}}_{aj} + \hat{\mathbf{F}}_{ej}. \quad (13)$$

A first contribution associated to the absorption of photons of the pump appears (5, 11):

$$\hat{\mathbf{F}}_{aj} = i\hbar \mathbf{k}_0 \frac{\Omega_0}{2} \left\{ \hat{\sigma}_j e^{i(\Delta_0 t - \mathbf{k}_0 \cdot \mathbf{r}_j)} - \text{h.c.} \right\}, \quad (14)$$

whereas the second contribution comes from the emission of the photons in any direction \mathbf{k} :

$$\hat{\mathbf{F}}_{ej} = i\hbar \sum_{\mathbf{k}} \mathbf{k} g_{\mathbf{k}} \left\{ \hat{a}_{\mathbf{k}}^\dagger \hat{\sigma}_j e^{i(\omega_{\mathbf{k}} - \omega_a)t - i\mathbf{k} \cdot \mathbf{r}_j} - \hat{\sigma}_j^\dagger \hat{a}_{\mathbf{k}} e^{-i(\omega_{\mathbf{k}} - \omega_a)t + i\mathbf{k} \cdot \mathbf{r}_j} \right\}. \quad (15)$$

In Eq. (15), the counter-rotating terms proportional to $\exp[\pm i(\omega_{\mathbf{k}} + \omega_a)t]$ were neglected.

As we are interested in comparing the radiation pressure force to the single-atom case, we define the average radiation force $\hat{\mathbf{F}} = (1/N) \sum_j \hat{\mathbf{F}}_j = (F_{tot}/N) \hat{\mathbf{e}}_z$ that measures acceleration of the cloud center-of-mass given by $\mathbf{a}_{CM} = \hat{\mathbf{F}}/m$, with m the single-atom mass. Note that this average force is N times smaller than the total force F_{tot} acting on the whole cloud of atoms. Since we consider clouds with rotational symmetry around the laser axis, this force is in the same direction as the incident field wave vector $\mathbf{k}_0 = k_0 \hat{\mathbf{e}}_z$. This average force is measured by time-of flight techniques in cold atomic clouds released, for instance, from magneto-optical traps (MOTs) and has recently revealed cooperative effects in the scattering by extended atomic samples (6, 18). As the scattered radiation, this force is an observable that contains signatures of the cooperative scattering by the atoms (5, 6). The average absorption force along the z -axis, resulting from the recoil received upon absorption of a photon from the incident laser, reads

$$\hat{F}_a = \frac{i}{2N} \hbar k_0 \Omega_0 \sum_{j=1}^N \left[\hat{\sigma}_j e^{i\Delta_0 t - i\mathbf{k}_0 \cdot \mathbf{r}_j} - \text{h.c.} \right]. \quad (16)$$

Similarly, the average emission force writes $\hat{\mathbf{F}}_e = (1/N) \sum_j \hat{\mathbf{F}}_{ej}$. Inserting the expression for $\hat{a}_{\mathbf{k}}$ from Eq. (4) into Eq. (15), and approximating the discrete sum over the modes \mathbf{k} by an integral,

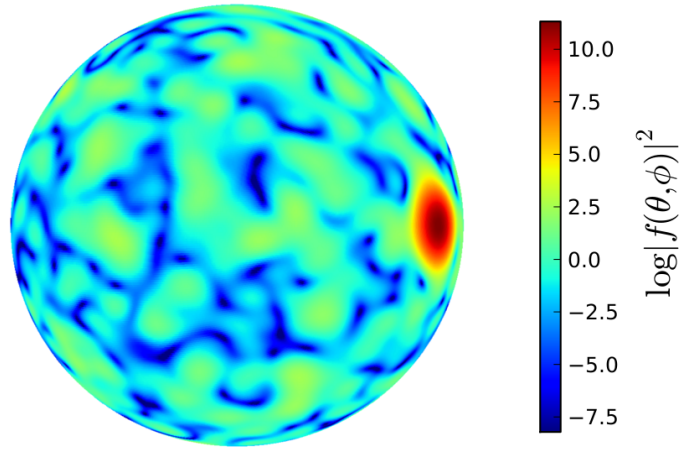


Figure 1. Scattered intensity $|f(\theta, \phi)|^2$ as given by Eq. (22) and Eq. (23) for a spherical cloud with a Gaussian density distribution of root mean square $10/k_0$. The number of scatterers is $N = 1000$, the detuning $\Delta_0 = 0$, and the incident field is coming from the left. The color-coded intensity is represented in log-scale. One can clearly see in red the strong forward emission of the sample, reminiscent of Mie scattering by clouds large compared to the wavelength. In the other directions, the scattered field is speckle-like due to the randomly positioned two-level scatterers, and describes the spontaneous emission of the cloud. Performing configuration averages would smooth out these fluctuations, except in the backward direction where, in the multiple scattering regime, the well known coherent backscattering cone is recovered (21, 22).

it is possible to obtain, as it was done for the radiation field operator \hat{E}_S of Eq. (7), the following expression for the average emission force along the z -axis (5):

$$\hat{F}_e = -\frac{\hbar k_0 \Gamma}{8\pi N} \int_0^{2\pi} d\phi \int_0^\pi d\theta \sin \theta \cos \theta \sum_{j,m=1}^N \left[e^{-i\mathbf{k} \cdot (\mathbf{r}_j - \mathbf{r}_m)} \hat{\sigma}_m^\dagger \hat{\sigma}_j + \text{h.c.} \right]. \quad (17)$$

Neglecting virtual photon contributions, the expectation values of the absorption and emission forces for state (2) are

$$\langle \hat{F}_a \rangle = -\frac{\hbar k_0 \Omega_0}{N} \sum_{j=1}^N \text{Im} \left[\beta_j e^{-i\mathbf{k}_0 \cdot \mathbf{r}_j} \right] \quad (18)$$

$$\begin{aligned} \langle \hat{F}_e \rangle &= -\frac{\hbar k_0 \Gamma}{4\pi N} \int_0^{2\pi} d\phi \int_0^\pi d\theta \sin \theta \cos \theta \sum_{j,m=1}^N \left[\beta_j \beta_m^* e^{-i\mathbf{k} \cdot (\mathbf{r}_j - \mathbf{r}_m)} \right] \\ &= -\frac{\hbar k_0 \Gamma}{N} \sum_{j,m=1}^N \frac{(z_j - z_m)}{|\mathbf{r}_j - \mathbf{r}_m|} j_1(k_0 |\mathbf{r}_j - \mathbf{r}_m|) \text{Im}(\beta_j \beta_m^*), \end{aligned} \quad (19)$$

where we used the identity

$$\int_0^{2\pi} d\phi \int_0^\pi d\theta \sin \theta \cos \theta e^{-i\mathbf{k} \cdot (\mathbf{r} - \mathbf{r}')} = 4\pi i \frac{z - z'}{|\mathbf{r} - \mathbf{r}'|} j_1(k_0 |\mathbf{r} - \mathbf{r}'|). \quad (20)$$

$j_1(z)$ here refers the first order spherical Bessel function. Note that the decomposition into absorption (18) and emission (19) forces is fully compatible with classical expressions of the optical force (19), where the force arises as the product between the atomic dipole and the *total* field (20) (i.e., including the radiation from the other atoms).

5. Optical Theorem

Let us now discuss the formulation of the optical theorem in the framework of collective scattering. In the far-field limit, the field is

$$E(\mathbf{r}) = \left[\frac{E_0}{2} e^{ikz} + E_s^{(\text{far})}(\mathbf{k}_z) \right] e^{-i\omega_0 t} = \frac{E_0}{2} \left[e^{ik_0 z} - \frac{e^{ik_0 r}}{k_0 r} f(\theta, \phi) \right] e^{-i\omega_0 t} \quad (21)$$

where the structure factor for the scattered field f is given by

$$f(\theta, \phi) = \frac{\Gamma}{\Omega_0} \sum_j \beta_j e^{-i\mathbf{k} \cdot \mathbf{r}_j}. \quad (22)$$

As a consequence, the scattered intensity at a large distance r from the cloud is

$$I_s = I_0 \frac{|f(\theta, \phi)|^2}{k_0^2 r^2}, \quad (23)$$

while the total scattering cross section reads

$$\sigma_{sca} = \frac{1}{k_0^2} \int_0^{2\pi} d\phi \int_0^\pi d\theta \sin \theta |f(\theta, \phi)|^2. \quad (24)$$

Figure 1 shows the emission diagram of the scattered field and for resonant excitation and a spherical cloud of atoms with a Gaussian density distribution. The energy conservation imposes that

$$\sigma_{ext} = \sigma_{sca} + \sigma_{abs} \quad (25)$$

where σ_{ext} and σ_{abs} are the cross sections for extinction and absorption, respectively. The extinction cross section is then obtained from the optical theorem. In the forward direction ($\theta = 0$) the total field is

$$E_{fwd} = \frac{E_0}{2} \left[e^{ik_0 z} - \frac{e^{ik_0 r}}{k_0 r} f(0) \right] e^{-i\omega_0 t}. \quad (26)$$

Hence, observing the field in a plane far from the atoms, the radius expands as $r \sim z + (x^2 + y^2)/2z$ and one obtains

$$E_{fwd} \approx \frac{E_0}{2} \left[1 - \frac{f(0)}{k_0 z} e^{ik_0(x^2 + y^2)/2z} \right] e^{i(k_0 z - \omega_0 t)}, \quad (27)$$

so the intensity reads

$$|E_{fwd}|^2 \approx \frac{|E_0|^2}{4} \left\{ 1 - \frac{2}{k_0 z} \text{Re} \left[f(0) e^{ik_0(x^2 + y^2)/2z} \right] \right\} \quad (28)$$

The measured intensity is the incident intensity minus the extinction intensity; in Eq. (28), the integration over x, y gives a factor $2i\pi z/k_0$, and one gets

$$\sigma_{ext} = -\frac{4\pi}{k_0^2} \text{Im}[f(0)] \quad (29)$$

Hence, from Eq. (25) one obtains the relation

$$-\text{Im}[f(0)] = \frac{1}{4\pi} \int_0^{2\pi} d\phi \int_0^\pi d\theta \sin\theta |f(\theta, \phi)|^2 + \frac{k_0^2}{4\pi} \sigma_{abs} \quad (30)$$

In our microscopic description of the light-atom interaction there is no absorption, so that $\sigma_{abs} = 0$. An illustration of the validity of the optical theorem is given in Figure 2 for resonant light scattering by a slab containing two-level scatterers with a uniform density distribution. From Eqs. (22) and (29), we obtain the relation

$$-\frac{\Omega_0}{\Gamma} \sum_j \text{Im} [\beta_j e^{-i\mathbf{k}_0 \cdot \mathbf{r}_j}] = \frac{1}{4\pi} \int_0^{2\pi} d\phi \int_0^\pi d\theta \sin\theta \sum_{j,m} [\beta_j \beta_m^* e^{-i\mathbf{k} \cdot (\mathbf{r}_j - \mathbf{r}_m)}] \quad (31)$$

Consequently, using Eqs. (18) and (19), the average force along the z -axis reads:

$$F_z = \frac{\hbar k_0 \Gamma}{4\pi N} \int_0^{2\pi} d\phi \int_0^\pi d\theta \sin\theta (1 - \cos\theta) \sum_{j,m=1}^N [\beta_j \beta_m^* e^{-i\mathbf{k} \cdot (\mathbf{r}_j - \mathbf{r}_m)}]. \quad (32)$$

We observe from Eq. (32) that the average radiation pressure force is not merely proportional to the excitation probability, i.e. $\sum_j |\beta_j|^2$, but it is the result of an interference between the different atomic dipoles β_j . For this reason a measurement of the force captures the coherence properties of the scattering process as well as the detection of the light intensity. To make this point more explicit, using Eq. (9), it is possible to write the force as

$$F_z = \frac{r^2}{Nc} \int_0^{2\pi} d\phi \int_0^\pi d\theta \sin\theta (1 - \cos\theta) I_s(\theta, \phi), \quad (33)$$

where the scattered far-field intensity is $I_s(\theta, \phi) = 2c\epsilon_0 |E_s(\theta, \phi)|^2$. This highlights the fact that the radiation pressure force, that pushes the atoms along the direction of the incident beam, is proportional to the net radiation flux of the scattered intensity.

In the case of an isotropic emission (e.g., single-atom case, or cloud much smaller than the wavelength), the scattered intensity I_s is independent on the direction and we get $F_z = (4\pi r^2 / (Nc)) I_s$: the direct proportionality between scattered power and radiation pressure force is recovered. The cooperative effect of light scattering in such small samples is then encoded in the total scattered intensity I_s . In the case of superradiant scattering for larger samples, a pronounced emission into the forward direction decreases the radiation force, as observed for example in Ref. (6).

6. Scaling of the scattering cross section

In this section we are interested in understanding how the scattering cross section scales with the parameters of the system. We consider the case of a slab with uniform density distribution. The slab contains N atoms and its size along the x , y , z axes is denoted by L_x , L_y , L_z respectively. The numerical simulations presented in figure 3 show how the scattering cross section depends on the optical thickness of the cloud $b_0 = 6\pi N / (k_0^2 L_x L_y)$. For dilute clouds of atoms we find:

$$\sigma_{sca} = 2.15 \times L_x L_y \left[1 - \exp\left(-\frac{0.63 b_0}{2.15}\right) \right]. \quad (34)$$

When the slab is optically thick, i.e. $b_0 \gg 1$, we observe that the cross section appears to approach $2 \times L_x L_y$. This factor of two corresponds to the well-known ‘‘extinction paradox’’

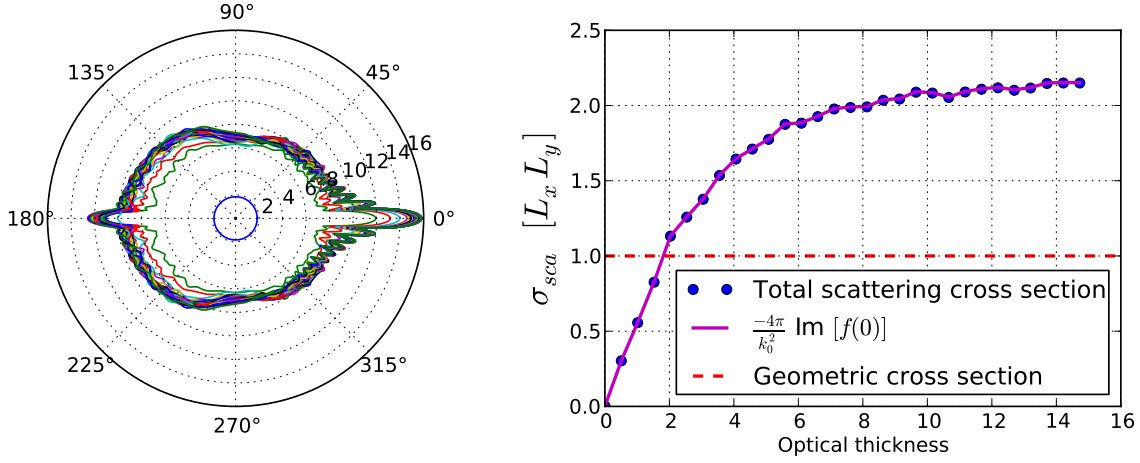


Figure 2. Illustration of the optical theorem. Left: the scattered intensity integrated along ϕ , i.e., $g(\theta) = \int_0^{2\pi} d\phi |f(\theta, \phi)|^2$, is shown for resonant light $\Delta_0 = 0$ and a slab geometry with a uniform density distribution. The number of atomic scatterers is varied between 1 and 5000 (from inside to outside curves). The transverse size of the slab is $L_{x,y} = 80/k_0$ and the longitudinal size is varied such that $L_z = (20/k_0)N/5000$. This procedure allows us to vary the optical thickness $b_0 = 6\pi N/(k_0^2 L_x L_y)$ between $3 \cdot 10^{-3}$ and 15 while maintaining the atomic density constant. The incident field is coming from the left and the intensity is plotted in log-scale. In addition to the forward Mie-like lobe, a lobe is also observed in the backward direction which we attribute to light reflection due to the sharp variation of optical index when the light hits the slab. Right: the blue circles represents the total scattering cross section obtained by integrating the emission diagram over θ and ϕ , i.e., $\sigma_{sca} = 1/k_0^2 \times \int_0^\pi d\theta \sin(\theta) g(\theta)$. In our microscopic model, there is no absorption so that $\sigma_{abs} = 0$, leading to $\sigma_{ext} = \sigma_{sca}$. The optical theorem Eq. (29) can thus be written as $\sigma_{sca} = -(4\pi/k_0^2) \text{Im}[f(0)]$, which is plotted in magenta. The good agreement between the two curves illustrates the validity of the optical theorem.

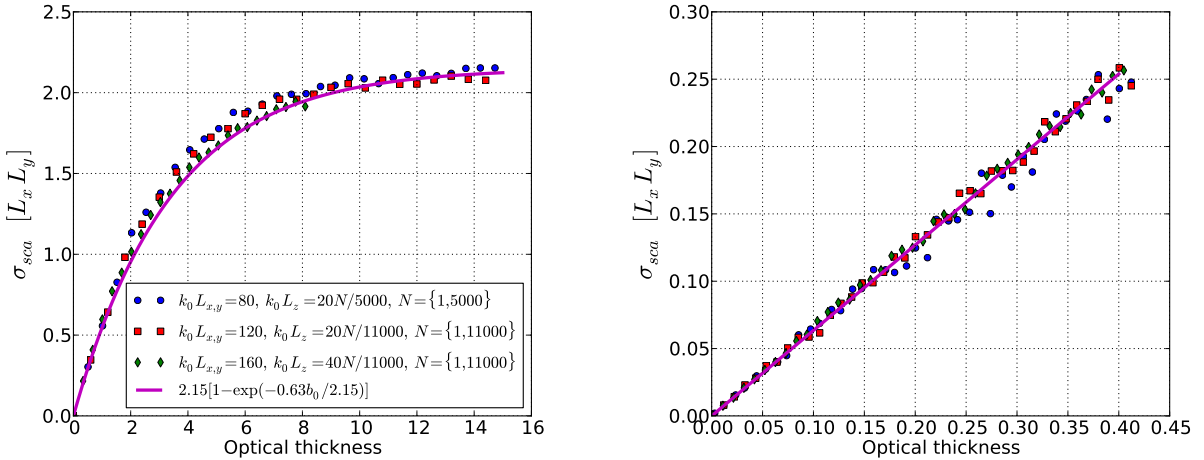


Figure 3. Scaling of the scattering cross section. Left plot: following the same procedure as the one described in figure 2, we compute the scattering cross sections for different slab geometries. The results are shown in scatter plot with different colors. The parameters of the simulations are reported in the legend of the figure. By fitting the data, constraining the slope in the limit $b_0 \rightarrow 0$ (right plot), we obtain a scattering cross section that scales with the optical thickness b_0 of the slab according to Eq. (34) (magenta full line).

(23, 24) for which the extinction cross section is twice as large as the one predicted by geometrical optics due to the diffraction contribution. The residual deviations from the factor of 2 between the scattering and geometrical cross sections might be associated to a still moderate size of our sample. For spherical dielectric spheres, σ_{ext} shows an oscillatory behavior around $2\sigma_{geo}$ ($\sigma_{geo} = L_x L_y$ for our square geometry), which is damped for increasing sizes of the sphere (25, 26). Furthermore, in the limiting case $b_0 \ll 1$ the scattering cross section can be written as $\sigma_{sca} = 0.63 \times (L_x L_y) b_0 = 0.63 \times N \sigma_0$, where $\sigma_0 = 3\lambda^2/(2\pi)$ is the resonant scattering cross section for a single atom, whereas for off-resonant excitation ($\Delta_0 = 3\Gamma$), we have found that $\sigma_{sca} = L_x L_y b(\Delta_0)$ (where $b(\Delta_0) = b_0/(1 + 4\Delta_0^2/\Gamma^2)$). A similar deviation in the case of a finite number of resonant dipoles has been noted in (27).

7. Conclusion

We here discussed the superradiant emission of a cloud of cold atoms, when the interference of the waves radiated by the atomic dipoles builds up a coherent emission. Despite the fact that the simple relation between absorbed photons and radiation pressure force existing in the single-atom case was lost, the optical theorem allowed to recover a simple relation between the total scattered intensity and the displacement of the cloud center-of-mass. The measure of the force of the center of mass of the atomic cloud contains (partial) information on the scattered intensity, even for large values of optical thickness of the cloud. We have computed the total scattering cross section which approaches a value close to twice the geometrical cross section of the sample, in line with the well-know extinction paradox. Further studies will include the precise role of the laser-atom detuning Δ_0 , as our results indicate that $b(\Delta_0)$ does not seem to be an universal single scaling parameter.

8. Acknowledgements

We acknowledge financial support from IRSES project COSCALI and from USP/COFECUB (projet Uc Ph 123/11). R. B. and Ph. W. C. acknowledge support from the Fundação de Amparo Pesquisa do Estado de São Paulo (FAPESP). M. T. R. is supported by an Averroès exchange program.

References

- (1) R. H. Dicke, Phys. Rev. **93**, 99 (1954).
- (2) R. Friedberg, S. R. Hartman, and J. T. Manassah, Phys. Rep. **7**, 101 (1973).
- (3) J. Keaveney, A. Sargsyan, U. Krohn, I. G. Hughes, D. Sarkisyan, and C. S. Adams, Phys. Rev. Lett. **108**, 173601 (2012).
- (4) R. Bachelard, Ph. W. Courteille, R. Kaiser, and N. Piovella, Europhys. Lett. **97**, 14004 (2012).
- (5) Ph. W. Courteille, S. Bux, E. Lucioni, K. Lauber, T. Bienaimé, R. Kaiser, and N. Piovella, Euro. Phys. J. D **58**, 69 (2010).
- (6) T. Bienaimé, S. Bux, E. Lucioni, Ph. W. Courteille, N. Piovella, and R. Kaiser, Phys. Rev. Lett. **104**, 183602 (2010).
- (7) G. K. Campbell, A. E. Leanhardt, J. Mun, M. Boyd, E. W. Streed, W. Ketterle, and D. E. Pritchard, Phys. Rev. Lett. **94**, 170403 (2005).
- (8) R. Bachelard, H. Bender, Ph. W. Courteille, N. Piovella, C. Stehle, C. Zimmermann, and S. Slama, Phys. Rev. A **86**, 043605 (2012).
- (9) M. O. Scully, E. Fry, C. H. R. Ooi, and K. Wodkiewicz, Phys. Rev. Lett. **96**, 010501 (2006).
- (10) A. A. Svidzinsky, J. T. Chang, and M. O. Scully, Phys. Rev. Lett. **100**, 160504 (2008).
- (11) R. Bachelard, N. Piovella, and Ph. W. Courteille, Phys. Rev. A **84**, 013821 (2011).
- (12) T. Bienaimé, M. Petruzzo, D. Bigerni, N. Piovella, and R. Kaiser, J. Mod. Opt. **58**, 1942 (2011).
- (13) A. A. Svidzinsky, J. T. Chang, and M. O. Scully, Phys. Rev. A **81**, 053821 (2010).
- (14) M. O. Scully and A. A. Svidzinsky, Phys. Lett. A **373**, 1283 (2009).
- (15) M. O. Scully and A. A. Svidzinsky, Science **328**, 1239 (2010).
- (16) R. Röhlberger, K. Schlage, B. Sahoo, S. Couet, and R. Rüffer, Science **328**, 1239 (2010).
- (17) S. Prasad, and R. J. Glauber, Phys. Rev. A **82**, 063805 (2010).
- (18) H. Bender, C. Stehle, S. Slama, R. Kaiser, N. Piovella, C. Zimmermann, and Ph. W. Courteille, Phys. Rev. A **82**, 011404 (2010).
- (19) N. Piovella, R. Bachelard and Ph. W. Courteille, J. of Plasma Phys., available on CJO. doi:10.1017/S0022377813000275 (2013).
- (20) J. P. Gordon, and A. Ashkin, Phys. Rev. A **21**, 1606 (1980).
- (21) M. P. van Albada, and A. Lagendijk, Phys. Rev. Lett. **55**, 2692 (1985).
- (22) P.-E. Wolf, and G. Maret, Phys. Rev. Lett. **55**, 2696 (1985).
- (23) H. C. Van de Hulst, "Light scattering by small particles", New York: Dover, p. 1038. (1981).
- (24) C. F. Bohren, and D. R. Huffman, "Absorption and scattering of light by small particles", New York: Wiley, p. 107-111, (1983).
- (25) S. G. Kargl, and P. L. Marston, J. Acoust. Soc. Am. **88** 1103 (1990).
- (26) M. J. Berg, C. M. Sorensen, and A. Chakrabarti, J. Quant. Spect. Rad. Tranf. **112**, 1170 (2011).
- (27) L. Chomaz, L. Corman, T. Yefsah, R. Desbuquois, and J. Dalibard, New J. Phys. **14**, 055001 (2012).